AGILE: GIScience Series, 7, 43, 2026. https://doi.org/10.5194/agile-giss-7-43-2026
Proceedings of the 29th AGILE Conference on Geographic Information Science, 16–19 June 2026.
Eds.: Evelyn Uuemaa, Alexander Kmoch, Holger Virro, and Simon Scheider
This contribution underwent peer review based on a full paper submission.
© Author(s) 2026. This work is distributed under the Creative Commons Attribution 4.0 License.

Integrating state-space models with map-matching to improve estimates of active travel motion

Corin Staves[1], Mads Paulsen[1], Xixi Wang[1], Laurent Cazor[1], Thomas Rasmussen[1]

[1] *Department of Technology Management and Economics, Technical University of Denmark*

Correspondence: Corin Staves (cedst@dtu.dk)

Abstract.

Active travel researchers often use satellite navigation data to investigate relationships between behaviour, infrastructure, environmental exposures, and/or health. These studies often employ map-matching algorithms to convert the raw waypoints into trajectories through a transport network. While less common, satellite navigation data can also be used to investigate motion characteristics such as variations in speed and acceleration, which is especially relevant for investigating safety and physical activity. Emerging literature has demonstrated the value in combining map-matching with motion characteristics, but current methods are unreliable on noisy data. We present an open-source framework that integrates state-space modelling and map-matching to produce precise trajectories and consistent motion profiles using satellite navigation data. Our methodology takes advantage of additional information provided the raw waypoints (e.g., speed, accuracy) and knowledge of physical motion to capture plausible active travel behaviour even with noisy and variable-quality data. Through several examples, we demonstrate how the integrated methodology can produce more accurate motion profiles and map-matched trajectories versus existing methods, which is especially beneficial for data from older devices. This framework aims to support active travel research particularly in safety, environmental epidemiology, and physical activity, by enabling investigators to take greater advantage of available satellite navigation and network data.

Submission Type. Model, algorithm, software

BoK Concepts. [GC3-11-2] Space-time dynamic reasoning

Keywords. Map-matching, Kalman filters, Active travel, Physical activity, GNSS

1 Introduction

Supporting active travel (walking and cycling) is a growing policy and interdisciplinary research focus spanning geoscience, urban planning, transport, and health. Active travel is increasingly promoted for improving physical activity while reducing the carbon impacts of transport. While the health and sustainability benefits of increasing active travel are well-recognised, trade-offs with safety and road pollutant inhalation cause these health impacts to be unequally distributed both spatially and socio-demographically.

Satellite navigation (GNSS) data has helped researchers better understand active travel behaviour. Smartphone apps with GNSS have modernised data collection in transport and physical activity surveys to more accurately capture walking and cycling in the context of everyday travel. Detailed GNSS traces can be linked with transport network and micro-geospatial data to understand the environments active travellers experience during their journeys. This linking can offer valuable information on health-relevant environmental exposures such as noise and pollutant inhalation (Woodcock et al., 2014). It can also help behavioural researchers understand and model the relationships between micro-environmental features (e.g., greenness and infrastructure) and the routes and modes active travellers choose (Broach & Dill, 2016; Basu et al., 2022).

While existing active travel research has harnessed the spatial detail in GNSS data, there has been less attention to its potential for understanding motion dynamics. Speed and acceleration patterns are important for understanding active travel behaviour and health. They affect the energy intensity of walking and cycling (Herrmann et al., 2024), consequently influencing physical activity and pollutant inhalation. Excessive stopping and starting makes cycling less attractive (Winters et al., 2010; Grudgings et al.,

2023), and acceleration dynamics are also indicative of cycling injury risks (Micucci & Sangermano, 2020). Motion dynamics depend on person-specific tolerances, abilities, and fitness (Ausri & Bigazzi, 2024), so the trade-offs between potential benefits and risks of active travel vary from person to person. Data on motion dynamics can help active travel planners decide who and where to target for designing effective and safe infrastructure.

We present a methodology and open-source framework for modelling active travel motion through a transport network using GNSS data. The methodology integrates state-space models and novel map-matching strategies to convert noisy GNSS traces into plausible moment-by-moment motion traces. In the results section, we demonstrate how the integrated methodology can produce more realistic motion profiles and map traces versus existing approaches.

2. Literature review

Investigations into motion dynamics for active users have traditionally involved small-scale experiments on specialised equipment. For walking, treadmill tests are commonly used to assess how energy expenditure varies with speed and incline (Brage et al., 2007). For cycling, Parkin and Rotherham (2010) attached bar-mounted tracking devices to bicycle handlebars to estimate the relationship between gradient, acceleration, heart rate, and cycling energy expenditure. Zaripov and Gavrilovs (2019) monitored acceleration and energy profiles of an electric bicycle to capture relationships between acceleration, motor power, and human power. Milan et al. (2025) used an instrumented bike with various treadmill tests to investigate e-bike safety.

Large-scale population studies typically simplify the motion characteristics of pedestrians and cyclists. Energy expenditure estimates often disregard the impact of acceleration and/or assume constant speeds (Woodcock et al., 2014; Staves et al., 2023). Studies that have explicitly considered acceleration have had to rely on modelled estimates rather than directly observed data (Cappelli et al., 2024; Cazor et al., 2025). Exceptions include Ma and Luo (2016) who used smartphone GNSS trajectories to understand and model bicycle motion, and Mohamed and Bigazzi (2019) who used smartphone GNSS trajectories to compare the dynamics and energy requirements of bikes and E-bikes. In these cases, motion was modelled in open 2D space without considering network constraints or features.

Map-matching techniques have evolved over several decades to convert noisy GNSS data into plausible trajectories on a transport network (Lamb & Thiébaux, 1999; Newson & Krumm, 2009; Millard-Ball et al., 2019). The dominant approach in the state-of-the-art is hidden Markov modelling (HMM), which models potential matches as a series of hidden states with corresponding observation and transition probabilities (Han, 2015). Traditionally these probabilities were based on distances, but various adaptions have emerged to improve matching accuracy and realism. Haunert & Budig (2012) incorporated potential off-road movements due to incomplete network data. Wöltche (2023) introduced an open-source algorithm with novel pre-processing, candidate search, and scoring strategies to improve accuracy. These existing implementations have primarily focused on motor vehicle traffic. In the context of active travel, Gao et al. (2024) introduced a cycle-oriented algorithm with speed constraints and scoring that varied by link type.

In separate but related work, state-space models and in particular Kalman filters have been applied extensively in vehicle and aviation navigation to estimate smooth trajectories using noisy GNSS data. Kalman filters can output reliable moment-by-moment estimates of position, speed, and acceleration in space. Applications for walk and cycle map-matching exist but focus on bespoke sensor arrays with small highly detailed networks (Harder et al., 2022; Perul & Renaudin, 2022). Kalman filtering on large-scale cycling GNSS data was employed by Ma and Luo (2016) however, as mentioned earlier, this was in open 2D space without map-matching.

While there has been substantial progress in accurately map-matching active trips and modelling their motion, these areas have mainly developed independently. Emerging cycling literature has demonstrated the advantage of doing both together; for example, to precisely estimate energy expenditure (Ausri & Bigazzi, 2024) and to explore the relationship between speed, infrastructure, and terrain (Maurer et al., 2025). These existing studies estimated map-matched dynamics crudely through distance-time differencing and then smoothing and/or discarding infeasible points. While this can be suitable for large aggregate analyses and/or very high-precision data, it poorly handles noisy data and causes potentially useful trajectories to be discarded. Our proposed methodology combines advances in map-matching and state-space models, taking greater advantage of the information provided in GNSS datapoints (i.e., including accuracy and speed through doppler shift) and our understanding of physical motion. We demonstrate how this framework can be used to model plausible and accurate motion estimates through a network with noisy and variable-quality data.

3. Methodology

The structure of the framework is given in Figure 1.

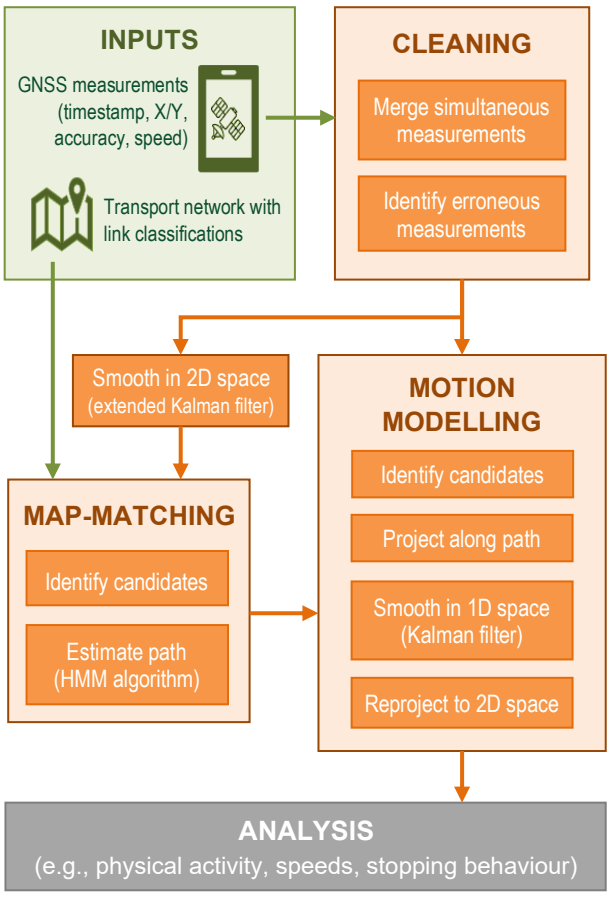

Figure 1 Integrated framework

3.1 Input data

The required inputs are:

1. Raw GNSS waypoints grouped into trips
2. Transport network

Raw waypoints should include position coordinates, timestamps, accuracy, and speed readings (where available) through doppler shift. These attributes can normally be obtained using smartphone data collection apps like motiontag (motiontag.com) and TravelVU (www.travelvu.app).

The network map can be a directed or undirected graph representation of the transport network for the mode(s) under investigation in geospatial data format. Network links can be enriched with classification data (e.g., on-road versus off-road cycle path) to facilitate more accurate matching. This data can often be obtained from OpenStreetMap (www.openstreetmap.org) using tools like OSMnx (Boeing, 2025).

3.2 Cleaning

A preliminary cleaning stage merges simultaneous measurements and remove clusters of clearly erroneous measurements.

To merge simultaneous measurements, readings with identical timestamps are combined into a single reading with average X/Y position, average speed, and maximum accuracy[1].

Erroneous measurements were identified through a two-step process. The first step identified outliers in the position-time differential between measurements in a 120-second moving window. After, sets of waypoints between outliers were flagged as erroneous clusters based on duration and distance from the rest of the trajectory.

3.3 Map-matching

Our map-matching algorithm builds from the open-source GraphLibrary repository (Forsch, 2020), written for Java, which applies Newson and Krumm's (2009) HMM methodology extended for off-road trajectories as described in Haunert & Budig (2012). We introduce several additional enhancements to take advantage of GNSS speed readings and more precisely estimate the paths active travellers use while minimising unrealistic detours and U-turns in the matched trajectory.

Smoothing in 2-dimensional space

To reduce GNSS measurement noise and irregularity before map-matching, the waypoints and speed estimates undergo a smoothing process. The smoothing procedure applies an extended Kalman filter in which the state vector contains X and Y position and their respective first derivatives. The measurement vector contains X, Y, and reported speed, and the measurement covariance depends on reported accuracy. The previously identified erroneous measurements are treated as missing datapoints.

Kalman filtering was performed using the Bayesian filters python library (Pearse, 2025). Full specifications of the Kalman filters are presented in a readme file in the corresponding GitHub repository (Section 3.5).

Identifying candidates

Following standard procedure, the first stage of map-matching identifies for each measurement the nearest point ('candidate') on nearby links. Our methodology then expands each measurement's candidate set to also include the candidates of nearby measurements. This minimises erroneous back-and-forth movements caused

[1] Higher accuracy values indicate greater uncertainty, so 'maximum' is a conservative estimate

by noisy measurements, especially when moving slowly. This enhancement is similar to the candidate adoption procedure described and illustrated in Wöltche (2023).

Enhanced transition costs

Transition costs traditionally consider routing distance alone. We expand this with three additional parameters. First, link-type penalty factors β_{h_l} are assigned so the matched path avoids link types unlikely to be used (e.g., footways if cycling), like in Gao et al. (2024). Second, to reduce unrealistic detours, we penalise deviations between the network distance and Euclidean distance between smoothed measurements. Third, to reduce unrealistic turning due to GNSS drift, we penalise deviations in the length and direction the matching lines.

The enhanced transition cost function between position i and subsequent position $j = i + 1$ is computed by

$$c_{ij} = \sum_{l \in P_{ij}} \beta_{h_l} x_l + \alpha \left[\beta_d d_{ij} + \beta_m \left(\frac{{z_{ij}}^{\parallel} + {z_{ij}}^{\perp}}{\Delta t_{ij}} \right) \right] \quad (1)$$

where P_{ij} is the least-cost path between i and j consisting of links l, α is the candidate cost weight as implemented in Forsch's (2020) algorithm, x_l is link length, β_{h_l} is a penalty factor based on the highway classification h_l of link l, and Δt_{ij} is the time difference between waypoints i and j. The difference d_{ij} between network and Euclidean distance is defined by

$$d_{ij} = \left| \left(\sum_{l \in P_{ij}} x_l \right)^2 - \left\| \boldsymbol{w}_j - \boldsymbol{w}_i \right\|_2^2 \right| \quad (2)$$

where $\boldsymbol{w}_i$ is the smoothed waypoint coordinate at position i. The corresponding coefficient is β_d.

Next, ${z_{ij}}^{\parallel}$ and ${z_{ij}}^{\perp}$ describe the parallel and orthogonal components of the deviation between matching lines $\boldsymbol{m}_i$ and $\boldsymbol{m}_j$ calculated by

$${z_{ij}}^{\parallel} = \left| \|\boldsymbol{m}_i\|_2^2 - \left(\frac{\boldsymbol{m}_i \cdot \boldsymbol{m}_j}{\|\boldsymbol{m}_i\|_2} \right)^2 \right| \quad (3)$$

$${z_{ij}}^{\perp} = \left(\frac{{\boldsymbol{m}_i}^{\perp} \cdot \boldsymbol{m}_j}{\|\boldsymbol{m}_i\|_2} \right)^2 \quad (4)$$

Where $\boldsymbol{m}_i$ is the vector from waypoint $\boldsymbol{w}_i$ to the respective candidate $\boldsymbol{c}_i$ on the network:

$$\boldsymbol{m}_i = \boldsymbol{c}_i - \boldsymbol{w}_i \quad (5)$$

The components ${z_{ij}}^{\parallel}$ and ${z_{ij}}^{\perp}$ capture changes in direction along the matched path relative to the GNSS trajectory. When both lines run parallel, these components become zero. The corresponding coefficient is β_m.

3.4 Motion modelling

This final module models the dynamics of traveller motion along the map-matched path including positions, speeds, and acceleration at the requested time intervals.

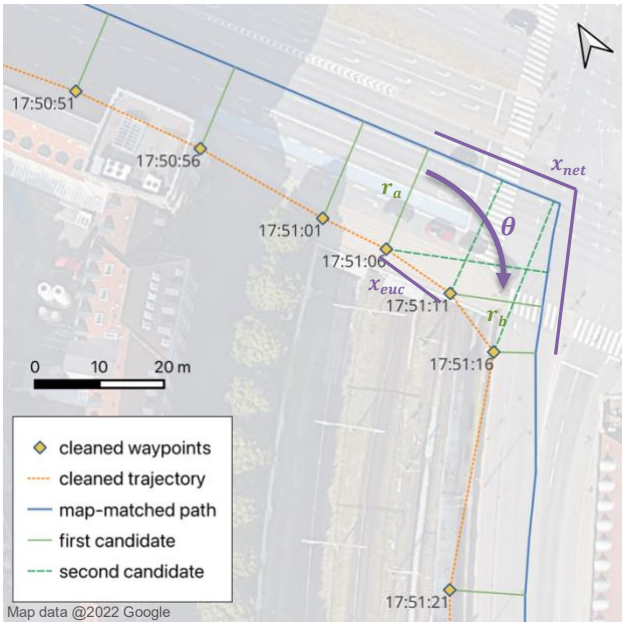

Figure 2 Sample of a cleaned and map-matched bike trajectory near a turn.

First, one or two candidate positions for each waypoint are identified along the path. This includes the nearest point on the path (i.e., the global minimum) and the second-nearest local minimum when the match is ambiguous (e.g., near corners), as shown in Figure 2.

After identifying candidates, the path and candidate positions are projected to one dimension. The projection explicitly handles discrepancies between map-matched and real distances travelled when turning, which occur due to simplifications of network links along road centrelines. While these discrepancies are minor at the macro-level, they cause unrealistic speed changes when turning (e.g., 'slingshot' movements) and consequently overestimations of acceleration and physical activity intensity at intersections. For each consecutive pair of measurements, the projected distance is given by

$$x_{proj} = x_{net} - (r_a + r_b) \tan\left(\frac{\theta}{2}\right) \geq x_{euc} \quad (6)$$

Where x_{euc} is the Euclidean distance between the measurements, x_{net} is the map-matched network distance between their nearest candidate positions, r_a and r_b are the candidate distances, and θ is the turning angle (i.e., the angle between lines linking measurements with their nearest candidates), as shown in Figure 2.

After projecting to one-dimensional space, trajectories are smoothed using a Kalman filter in which the state vector

consists of position, speed, and acceleration. The measurement vector contains the candidate position(s) and measured speed, and the measurement covariance depends on reported accuracy and candidate distance(s).

In the final stage, the modelled motion is re-projected back to two-dimensional space along the map-matched path.

3.5 Data and software availability

This framework is open-source and written in Python and Java. It is available at https://github.com/MobiJoule/activetravelmotion with an enclosed README.md file containing further technical details of the enclosed framework. The Kalman filter specifications are described in script/filter/README.md within this repository.

4. Example results

This section demonstrates our methodology for a sample of cycling trajectories collected from smartphones. Network data was obtained from OSM including all link types that could realistically carry cyclists. For this analysis, parameters and cost coefficients were calibrated manually through trial and error using a selection of trajectories. The link-type penalties β_{h_l} were set to 1.25 for car links where a parallel cycle track exists alongside, 1.4 for links where cycling is not allowed, and 10 for steps. The distance penalty β_d and match deviation penalty β_m were set to 0.6 and 1.4 respectively. The candidate cost weight α was set to 0.01.

4.1. Comparison of processing stages

Figures 3 and 4 present estimated speeds, accelerations, and trajectories at each processing stage for a part of a bicycle trip obtained from an iPhone 13. Figure 3 compares the modelled estimates (in red) against simpler measures of speed and acceleration based on first- and second-differencing positions. Cleaning removed the worst outliers, but cleaned results remain jagged with implausible peaks and variations when using these simpler measures. While these could be further smoothed independently, like in Auri and Bigazzi (2024), the estimated speeds and acceleration can be inconsistent and vulnerable to lateral noise in the waypoint positions. This can cause unrealistic energy expenditure estimates unless the noisy data are discarded.

Figure 4 visualises this same trajectory sample on the network. Figure 4i shows the raw waypoints, of which some are simultaneous, missing speeds, and/or clearly erroneous. Figure 4ii shows the cleaned trajectory, with simultaneous points merged and erroneous points removed (marked '×'). In the next stage (Figure 4iii), the waypoints are smoothed using a 2D Kalman filter and these smoothed points are map-matched to the network. Finally, Figures 4iv and 4v present the modelled speed and acceleration at one-second time intervals along the map-matched path. Despite the noisy input, the speed and acceleration values follow plausible behaviour; for example, slower speeds leading up to a bridge at 18:03:20, and then a brief acceleration as the cyclist rides downhill off the bridge.

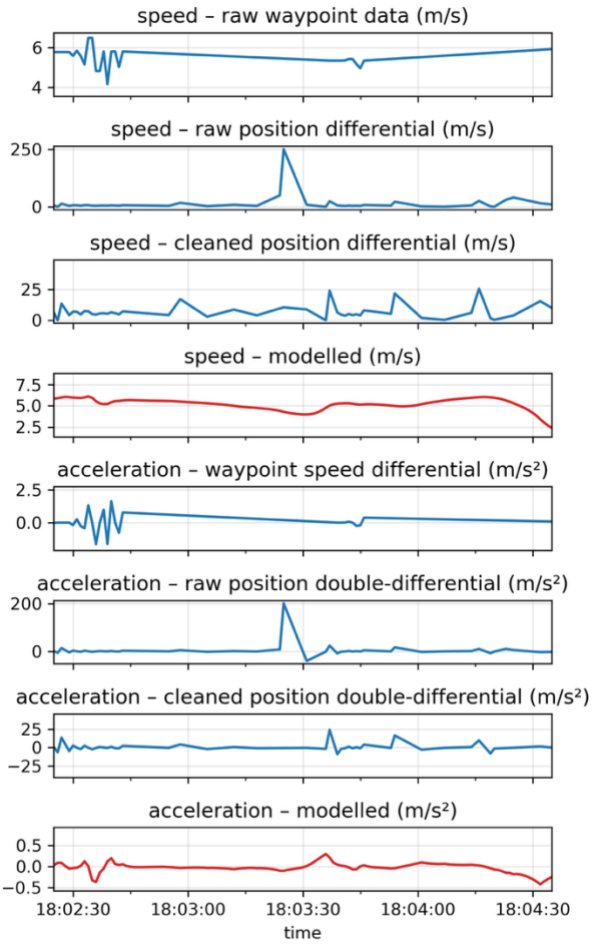

Figure 3 Comparison of speed and acceleration estimates

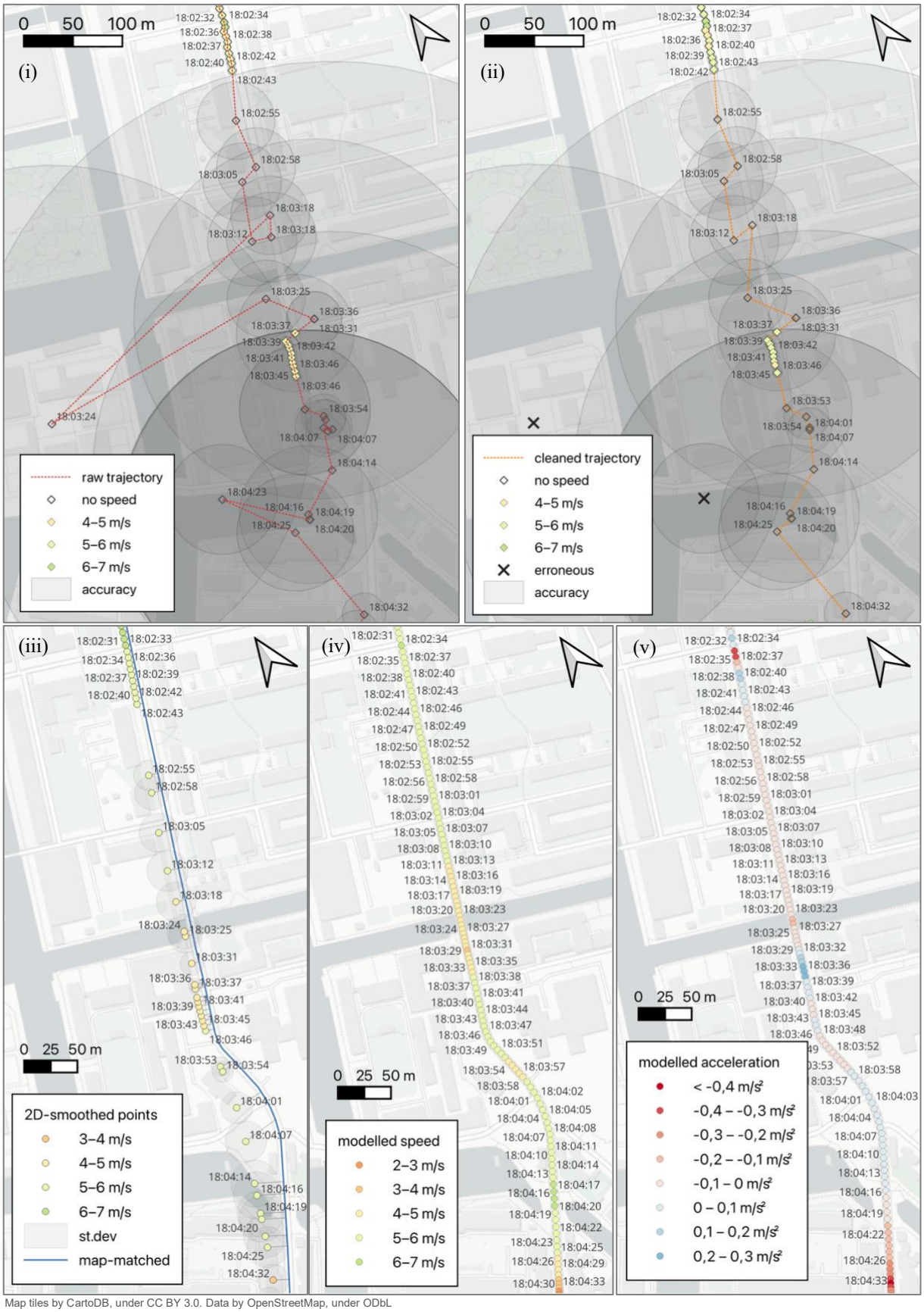

Map tiles by CartoDB, under CC BY 3.0. Data by OpenStreetMap, under ODbL

Figure 4 Example waypoint and trajectory data at each processing stage: (i) raw (ii) cleaned (iii) smoothed and map-map-matched (iv) final modelled speed (v) final modelled acceleration

4.2. Comparison of map-matching methods

Figure 5 compares the enclosed map-matching methodology with Haunert & Budig's (2012) algorithm and the matched route from a smartphone application. Due to significant lateral drift in these GNSS waypoints, both alternatives create deviating trajectories to minimise distances from the points to the path. However, both alternatives are implausible as they would imply exceptionally large speeds and accelerations as the cyclist moves through them. This would create inaccurate environmental exposure estimates away from the main road and exceptionally large energy expenditure estimates, likely causing these measurements to be discarded.

The enclosed method penalises deviations between Euclidean and path distance to reduce unrealistic detours. It also penalises deviations between consecutive matching lines to reduce unrealistic direction changing. Both penalties help to avoid implausible movements leading to a more accurate match, especially in the presence of GNSS drift.

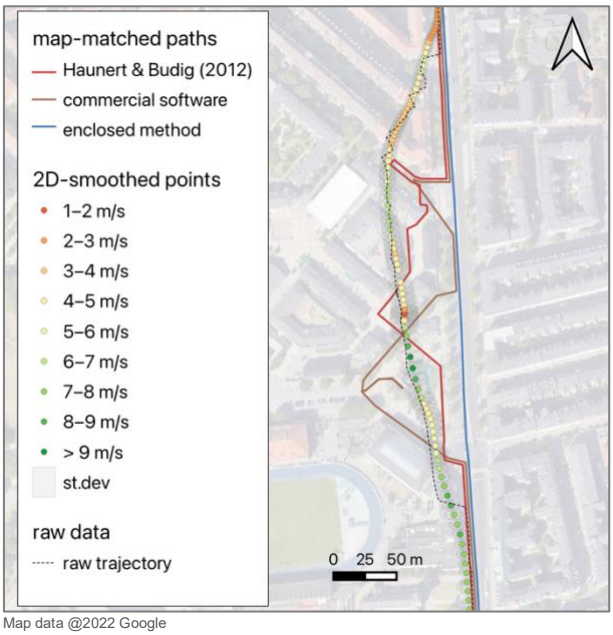

Map data @2022 Google

Figure 5 Example comparison of map-matching methods with GNSS drift

4.3. Comparison of aggregate distributions

Figure 6 explores the distributions of modelled speeds and accelerations for 8 smartphone users with 3+ hours each of urban conventional bicycle travel. The modelled speeds are compared against a baseline in which speed and acceleration are estimated using position-differentials from the raw GNSS dataset. There is substantial heterogeneity in observed behaviour for different users, which is consistent with previous findings (Maurer et al., 2025). For some cyclists, baseline distributions aligned well with modelled estimates, but for others results were inconsistent. Handset type played a large role, with the closest estimates coming from users with more modern devices (including Samsung A56 and iPhone 16), and the poorest baseline estimates coming from older devices (including Samsung A13 and iPhone 13).

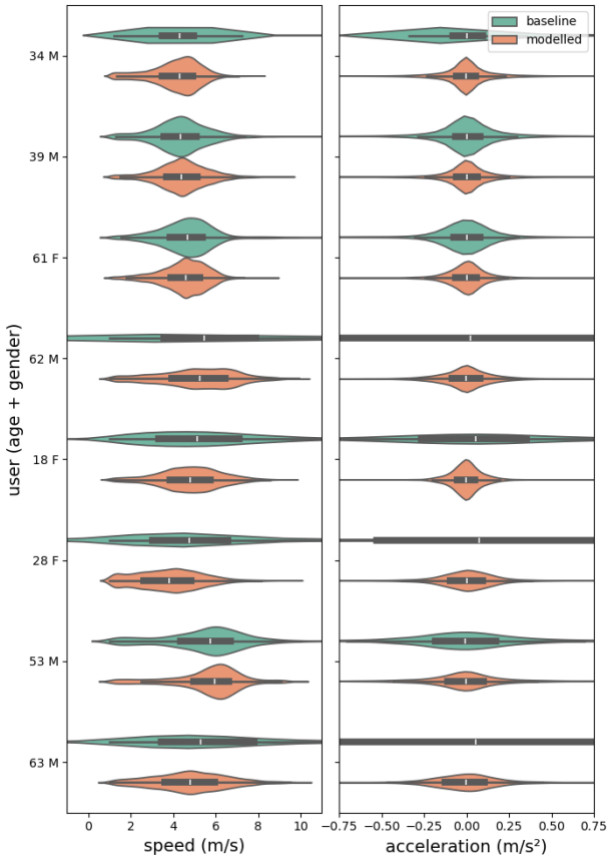

Figure 6 Speed and acceleration estimates for 8 cyclists using raw and modelled data

Physical activity estimates depend strongly on speed and acceleration (Wilson & Schmidt, 2020). This comparison highlights the value of the enclosed framework for producing realistic estimates of motion dynamics for assessing energy expenditure, especially when working with older devices.

5. Discussion

This paper demonstrates the potential for combining state-space models with advanced map-matching algorithms to model active travel motion on a transport network with high precision. The examples presented deal with cycling, but the framework can also be applied to walking by modifying the network and link penalties β_l.

Our methodology is intended for applications where it is advantageous to have detailed motion profiles linked with transport infrastructure, including road safety, transport mode and route choice, physical activity, and

environmental epidemiology. In contrast with current approaches that capture motion dynamics without network constraints, or use crude (e.g., distance-differenced) motion estimates on a map-matched network, the proposed methodology can capture realistic motion profiles through a network even for noisy and mixed-quality GNSS data. This can be especially valuable when working with older devices, smaller sample sizes, or panel datasets where it is important to preserve as much information as possible.

The enclosed analysis is demonstrative and qualitative, limited by a small dataset. As more data is collected, it could be feasible to perform quantitative benchmarking of map-matched routes like in Wöltche (2023) and Gao et al. (2024).

The code repository is under active development and continues to be refined as it is tested on additional GNSS datasets and use-cases. There is considerable potential to advance this framework to better model motion. The current framework is sequential and applies simple Kalman filter implementations that do not take full advantage of our knowledge of GNSS data or physical movement especially for bicycles. It does not incorporate lateral or vertical acceleration to ensure realistic motion dynamics through turns or slopes. For cycling, it could be more realistic to model energy expenditure directly using an advanced state-space representation that incorporates the kinematics of bicycle movement. Finally, a 'tighter' integration of map-matching with state-space modelling could provide a more elegant and robust framework that avoids multiple sequential processing stages. Such an integration could apply Kalman filters directly inside the HMM routine like in Lamb and Thiébaux (1999), and/or explicitly model GNSS drift like in Hu et al. (2010). While the current framework combines open-source packages in two programming languages (state-space models in Python and map-matching in Java), a more integrated and user-friendly framework could be written within a single programming language and repository.

Declaration of Generative AI in writing

The authors declare that they have *not* used generative AI tools in the preparation of this manuscript.

Acknowledgement

We thank the Independent Research Fund Denmark (DFF) for funding this research through the project "Human energy expenditure in mobility" (Grant ID: 2067-00077B)

References

Ausri, F., & Bigazzi, A. (2024). Mesoscopic model of cycling trip energy expenditure based on operating modes. *Journal of Cycling and Micromobility Research*, *2*, 100030. https://doi.org/10.1016/j.jcmr.2024.100030

Basu, N., Haque, Md. M., King, M., Kamruzzaman, Md., & Oviedo-Trespalacios, O. (2022). A systematic review of the factors associated with pedestrian route choice. *Transport Reviews*, *42*(5), 672–694. https://doi.org/10.1080/01441647.2021.2000064

Boeing, G. (2025). Modeling and Analyzing Urban Networks and Amenities With OSMnx. *Geographical Analysis*, *57*(4), 567–577. https://doi.org/10.1111/gean.70009

Brage, S., Ekelund, U., Brage, N., Hennings, M. A., Froberg, K., Franks, P. W., & Wareham, N. J. (2007). Hierarchy of individual calibration levels for heart rate and accelerometry to measure physical activity. *Journal of Applied Physiology*, *103*(2), 682–692. https://doi.org/10.1152/japplphysiol.00092.2006

Broach, J., & Dill, J. (2016). Using Predicted Bicyclist and Pedestrian Route Choice to Enhance Mode Choice Models. *Transportation Research Record: Journal of the Transportation Research Board*, *2564*(1), 52–59. https://doi.org/10.3141/2564-06

Cappelli, G., D'Apuzzo, M., Nardoianni, S., & Nicolosi, V. (2024). Exploring the Influences of Safety and Energy Expenditure Parameters on Cycling. *Sustainability*, *16*(7), 2739. https://doi.org/10.3390/su16072739

Cazor, L., Duncan, L., Isenschmid, U., Rasmussen, T., Staves, C., & Paulsen, M. (2025). *The impact of energy expenditure on cyclists' route choices: Model formulation and large-scale GPS case study*. Working paper.

Forsch, A. (2020). *GraphLibrary* [Computer software]. University of Bonn. https://gitlab.igg.uni-bonn.de/graphlibrary

Gao, T., Daamen, W., Krishnakumari, P., & Hoogendoorn, S. (2024). Map-matching for cycling travel data in urban area. *IET Intelligent Transport Systems*, *18*(11), 2178–2203. https://doi.org/10.1049/itr2.12567

Grudgings, N., Hughes, S., & Hagen-Zanker, A. (2023). What aspects of traffic intensity most influence cycling mode choice? A study of commuting in Surrey, UK. *International Journal of Sustainable Transportation*, *17*(2), 136–147. https://doi.org/10.1080/15568318.2021.1999539

Han, L. (2015). *Algorithm Design and Implementation of Map Matching of City-wide Floating Car Data*. Technische Universität München.

Harder, D., Shoushtari, H., & Sternberg, H. (2022). Real-Time Map Matching with a Backtracking Particle Filter Using Geospatial Analysis. *Sensors*, *22*(9), 3289. https://doi.org/10.3390/s22093289

Haunert, J.-H., & Budig, B. (2012). An algorithm for map matching given incomplete road data. *Proceedings of the 20th International Conference on Advances in Geographic Information Systems*, 510–513. https://doi.org/10.1145/2424321.2424402

Herrmann, S. D., Willis, E. A., Ainsworth, B. E., Barreira, T. V., Hastert, M., Kracht, C. L., Schuna, J. M., Cai, Z., Quan, M., Tudor-Locke, C., Whitt-Glover, M. C., & Jacobs, D. R. (2024). 2024 Adult Compendium of Physical Activities: A third update of the energy costs of human activities. *Journal of Sport and Health Science*, *13*(1), 6–12. https://doi.org/10.1016/j.jshs.2023.10.010

Lamb, P., & Thiébaux, S. (1999). *Avoiding Explicit Map-Matching in Vehicle Location*. 6th World Conference on Intelligent Transportation Systems.

Ma, X., & Luo, D. (2016). Modeling cyclist acceleration process for bicycle traffic simulation using naturalistic data. *Transportation Research Part F: Traffic Psychology and Behaviour*, *40*, 130–144. https://doi.org/10.1016/j.trf.2016.04.009

Maurer, L. F., Meister, A., & Axhausen, K. W. (2025). Cycling speed profiles from GPS data: Insights for conventional and electrified bicycles in Switzerland. *Journal of Cycling and Micromobility Research*, *5*, 100077. https://doi.org/10.1016/j.jcmr.2025.100077

Micucci, A., & Sangermano, M. (2020). A Study on Cyclists behaviour and bicycles Kinematic. *International Journal of Transport Development and Integration*, *4*(1), 14–28. https://doi.org/10.2495/TDI-V4-N1-14-28

Milan, P., Fah, Y. F., Feng, Z., Hong, X., & Diew, W. Y. (2025). Evaluating the safety of small-wheeled micro-mobility devices: A design-agnostic, performance-based experimental approach. *Transportation Research Interdisciplinary Perspectives*, *31*, 101376. https://doi.org/10.1016/j.trip.2025.101376

Millard-Ball, A., Hampshire, R. C., & Weinberger, R. R. (2019). Map-matching poor-quality GPS data in urban environments: The pgMapMatch package. *Transportation Planning and Technology*, *42*(6), 539–553. https://doi.org/10.1080/03081060.2019.1622249

Mohamed, A., & Bigazzi, A. (2019). Speed and road grade dynamics of urban trips on electric and conventional bicycles. *Transportmetrica B: Transport Dynamics*, *7*(1), 1467–1480. https://doi.org/10.1080/21680566.2019.1630691

Newson, P., & Krumm, J. (2009). Hidden Markov map matching through noise and sparseness. *Proceedings of the 17th ACM SIGSPATIAL International Conference on Advances in Geographic Information Systems*, 336–343.

Parkin, J., & Rotheram, J. (2010). Design speeds and acceleration characteristics of bicycle traffic for use in planning, design and appraisal. *Transport Policy*, *17*(5), 335–341. https://doi.org/10.1016/j.tranpol.2010.03.001

Pearse, G. (2025). *Bayesian Filters* (Version 1.4.5) [Computer software].

Perul, J., & Renaudin, V. (2022). BIKES: Bicycle Itinerancy Kalman Filter With Embedded Sensors for Challenging Urban Environment. *IEEE Sensors Journal*, *22*(6), 5270–5277. https://doi.org/10.1109/JSEN.2021.3086004

Staves, C., Zhang, Q., Woodcock, J., & Moeckel, R. (2023, January 9). *Integrating Health Effects within an Agent-based Land Use/Transport Model*. 102nd Annual Meeting of the Transportation Research Board.

Wilson, D. G., & Schmidt, T. (2020). *Bicycling Science* (Forth edition). The MIT Press.

Winters, M., Brauer, M., Setton, E. M., & Teschke, K. (2010). Built Environment Influences on Healthy Transportation Choices: Bicycling versus Driving. *Journal of Urban Health*, *87*(6), 969–993. https://doi.org/10.1007/s11524-010-9509-6

Wöltche, A. (2023). Open source map matching with Markov decision processes: A new method and a detailed benchmark with existing approaches. *Transactions in GIS*, *27*(7), 1959–1991. https://doi.org/10.1111/tgis.13107

Woodcock, J., Tainio, M., Cheshire, J., O\textquoterightBrien, O., & Goodman, A. (2014). Health effects of the London bicycle sharing system: Health impact modelling study. *BMJ*, *348*. https://doi.org/10.1136/bmj.g425

Xu, H., Liu, H., Tan, C.-W., & Bao, Y. (2010). Development and Application of an Enhanced Kalman Filter and Global Positioning System Error-Correction Approach for Improved Map-Matching. *Journal of Intelligent Transportation Systems*, *14*(1), 27–36. https://doi.org/10.1080/15472450903386013

Zaripov, R., & Gavrilovs, P. (2019). Study of dynamic characteristics of electric bicycles. *Procedia Computer Science*, *149*, 307–313. https://doi.org/10.1016/j.procs.2019.01.140